Single-Antenna ESP32-S3 Wi-Fi Angle Estimation Limits

Volodymyr Pavlenko
Lviv Polytechnic National University
Lviv, Ukraine
volodymyr.v.pavlenko@lpnu.ua

***Abstract*—Low-cost ESP32-class channel state information capture enables embedded Wi-Fi sensing studies, but trustworthy azimuth-estimation results depend on evaluation discipline and repeated-session structure. This paper studies a single-antenna ESP32-S3 setup for azimuth sensing in a controlled line-of-sight environment as a compact reference for broader low-cost embedded azimuth research. The dataset contains 4796 valid packets from 16 capture subsets, 2 experiments, and 8 nominal angle points. Four lightweight regressors are compared: RSSI linear, RSSI polynomial, CSI-kNN, and CSI+RSSI-kNN. Evaluation uses two experiment-wise folds that train on one experiment and test on the other, so all 8 angles are assessed out of fold. The CSI pipeline uses summary statistics and train-only PCA. Across pooled out-of-fold predictions, CSI-kNN reaches the best overall MAE of 73.8 deg and the best within-10-degree rate of 28.1%, while CSI+RSSI-kNN follows closely at 75.4 deg and 27.3%. The angle-wise results show pronounced sector dependence across the full circle: the present geometry captures exploitable directional structure at some azimuths, but the error remains large in several sectors and does not yet support stable practical azimuth sensing. These quantitative bounds provide a reproducible reference for further research on embedded azimuth estimation, alternative sensing geometries, coordinated low-cost receivers, and stricter repeated-session study designs.**

***Index Terms*—Wireless LAN (IEEE 802.11); Channel state information; Embedded systems.**

I. Introduction

Low-cost ESP32-class channel state information capture supports embedded Wi-Fi sensing on resource-constrained hardware [1]–[3]. For azimuth sensing, the central question is what angular information a single-antenna ESP32-S3 measurement geometry exposes when metadata integrity is kept visible and evaluation leakage is controlled. The same question also defines a reference point for broader research on low-cost embedded azimuth sensing, including coordinated multi-receiver configurations and richer measurement geometries.

Prior CSI/RSSI localization papers, broader CSI capability studies, and commodity-WLAN AoA systems demonstrate that stronger positional or angular performance is possible when the sensing surface is richer than the one studied here. In the cited literature, that richer sensing surface comes from different sources: hybrid CSI/RSSI fingerprints and signal preprocessing in WLAN localization [4], location-independent multi-node CSI/RSSI fusion for indoor tracking [5], broader multi-environment CSI evaluation campaigns [6], or AoA-oriented observation models with stronger geometric constraints [7], [8]. An adjacent ESP32-S3 publication on indoor ranging showed that the same device class can already support controlled, repeatable wireless measurements for distance estimation [9]. The present paper addresses the complementary azimuth question within the same low-cost embedded setting.

The study addresses this question through an integrity-aware, leakage-safe characterization of a low-cost single-antenna ESP32-S3 setup in a controlled LoS environment. The main elements are:

- a controlled LoS ESP32-S3 single-antenna study with 4796 valid packets across 16 capture subsets, 2 experiments, and 8 nominal angle points;
- experiment-wise evaluation that trains on one experiment and tests on the other, then reverses the roles, so the full 8-angle set is evaluated out of fold;
- a comparison of RSSI linear, RSSI polynomial, CSI-kNN, and CSI+RSSI-kNN under constrained embedded hardware;
- quantitative bounds on the present measurement geometry, including experiment-to-experiment variation and angle-dependent behavior across the full azimuth circle.

II. Research Scope and Goals

This study addresses a narrow question: what azimuth-estimation capability can be documented for this specific single-antenna ESP32-S3 geometry when the full angle set is evaluated under experiment-wise generalization rather than packet-randomized reuse? The study scope is restricted to one access point, one single-antenna receiver, one room, one LoS scenario, and two experiments. Within that scope, the study characterizes the present single-node configuration under a full-angle experiment-wise protocol and provides a reference result for broader work on embedded azimuth sensing. This role includes coordinated multi-node single-antenna studies, but it is not limited to them. This role also connects the paper to the adjacent ESP32-S3 ranging publication [9], which addressed a different observable under the same controlled-embedded methodology.

This scope is intentionally different from work that pursues the best attainable localization accuracy with richer sensing surfaces. A single-antenna ESP32-S3 receiver cannot expose the phase-difference information used by array-based AoA systems, and it does not inherit the calibration surface of denser CSI/RSSI fingerprinting deployments by default. The

TABLE I. STUDY CONFIGURATION AND EVALUATION SUMMARY

Aspect	Configuration
Geometry	Controlled LoS, 1 access point near room center, 1 single-antenna ESP32-S3 receiver on a nominal 2 m circular trajectory, 8 nominal azimuth marks: 0, 45, 90, 135, 180, 225, 270, 315 deg
Acquisition	2.4 GHz ESP32-S3 CSI send/receive workflow; fixed receiver orientation; 0 deg toward the access point, clockwise positive; 300 packets per angle per experiment; 16 capture subsets; 2 experiments; 4796 valid packets
Evaluation	Experiment-wise leave-one-experiment-out over the experiment label; fold 1 trains on experiment 002 and tests on experiment 001 (2399/2397 packets), fold 2 trains on experiment 001 and tests on experiment 002 (2397/2399 packets); all 8 angles are evaluated out of fold
Models	RSSI linear and second-order polynomial regressors; standardized distance-weighted CSI-kNN and CSI+RSSI-kNN with $k = 7$
Features	CSI summary features based on mean, standard deviation, median, top-decile mean amplitude, and the number of CSI subcarrier pairs, followed by train-only PCA over the first three components; the fused model adds packet RSSI and experiment-angle median RSSI; fold-wise explained ratios are (0.9028, 0.0547, 0.0204) and (0.7820, 0.1085, 0.0786)
Metrics	Wrapped-angle MAE, RMSE, MedAE, within-10-degree rate ($P10$), signed bias

appropriate claim is therefore a controlled capability characterization of this measurement geometry and its current applicability limits.

III. EXPERIMENTAL SETUP AND EVALUATION

The experiment was designed as a controlled single-node LoS study under one fixed geometry. It used one access point near the room center and one single-antenna ESP32-S3 receiver moved over a nominal 2 m circular trajectory at 8 azimuth marks: 0, 45, 90, 135, 180, 225, 270, and 315 deg. The receiver orientation was kept fixed; 0 deg denotes the receiver front axis toward the access point, and positive rotation is clockwise. The acquisition used the ESP32-S3 CSI send/receive workflow on 2.4 GHz Wi-Fi and targeted 300 packets per angle per experiment. The evidence package covers one LoS scenario, 2 experiments, and 16 capture subsets. After parsing and validity checks, 4796 packets remained for analysis [10].

Table I summarizes the fixed study design. The evaluation is experiment-wise rather than packet-random: one fold trains on experiment 002 and tests on experiment 001, and the second fold reverses the roles. Each test fold therefore contains the full 8-angle set. In this paper, integrity-aware evaluation denotes that experiment labels were standardized at the capture-subset level before the experiment-wise split was formed, so train and test remain separated by experiment.

Four lightweight regressors were compared: RSSI linear, RSSI polynomial, CSI-kNN, and CSI+RSSI-kNN. The CSI-based regressors used standardized distance-weighted kNN with $k = 7$. The CSI feature pipeline used summary descriptors of the CSI amplitude profile together with train-only PCA; the fused model added packet-level and experiment-angle-median RSSI information. All angle-error metrics were computed from wrapped circular differences between the predicted and true azimuth, so MAE, RMSE, MedAE, and $P10$ reflect circular error rather than linear degree subtraction. Evaluation reports MAE, RMSE, MedAE, and the within-10-degree hit rate, together with signed bias. Across the two folds, the first three train-only PCA components explained (0.9028, 0.0547, 0.0204) and (0.7820, 0.1085, 0.0786).

TABLE II. EXPERIMENT-WISE PERFORMANCE ON 4796 POOLED OUT-OF-FOLD PREDICTIONS. $P10$ IS THE SHARE WITH ABSOLUTE ERROR NOT LARGER THAN 10 DEG.

Method	MAE	RMSE	MedAE	$P10$	Bias
CSI-kNN	73.8	94.0	90.0	28.1%	-6.1
CSI+RSSI-kNN	75.4	95.3	90.0	27.3%	-8.9
RSSI poly2	94.0	109.4	93.9	5.1%	-5.0
RSSI linear	94.0	109.9	86.7	8.9%	0.6

TABLE III. CROSS-EXPERIMENT MAE BY HELD-OUT EXPERIMENT

Method	Hold-out experiment 001	Hold-out experiment 002
CSI-kNN	70.4	77.1
CSI+RSSI-kNN	69.4	81.4
RSSI poly2	86.2	101.8
RSSI linear	86.4	101.7

IV. QUANTITATIVE RESULTS

Table II reports pooled out-of-fold error metrics over both experiment-wise folds. CSI-kNN gives the lowest MAE at 73.8 deg and the highest within-10-degree rate at 28.1%. CSI+RSSI-kNN follows closely at 75.4 deg MAE and 27.3% within 10 deg. The RSSI regressors remain near 94.0 deg MAE. Figures 1 and 2 show the same result at the structural and angle-wise levels.

The fold-level view in Table III shows that the two CSI-based methods remain strongest in both held-out experiments, but their MAE still varies between 69.4 deg and 81.4 deg across folds. This experiment-wise gap remains large enough to show that the present geometry is still sensitive to experiment-to-experiment variation.

The behavior is clearer in Figure 1. The CSI-based models recover local structure around some nominal angles, especially near 0, 90, and 315 deg, but substantial overlap remains across 45, 135, 180, 225, and 270 deg. The same point is quantified in Figure 2. CSI+RSSI-kNN gives 17.7 deg MAE at 0 deg and 24.1 deg at 90 deg, while CSI-kNN gives 28.7 deg at 315 deg. However, CSI-kNN also reaches 155.3 deg MAE at 180 deg and 117.5 deg at 270 deg. The RSSI models remain weaker in aggregate, yet they are comparatively lower at 135 deg and 180 deg than the CSI methods. The present geometry therefore carries directional information, but that information is strongly sector-dependent rather than uniform over the full circle.

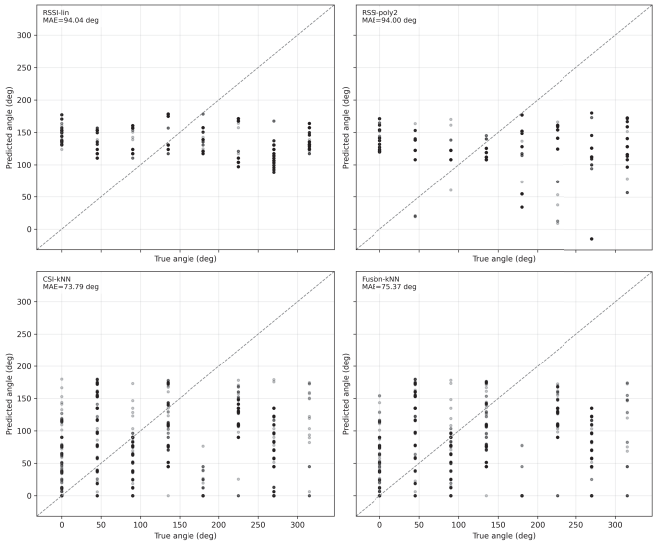

Fig. 1. Pooled out-of-fold predicted-versus-true-angle scatter plots for the 4 evaluated regressors. The CSI-based models recover local structure at some angles, but substantial overlap remains over the full azimuth circle.

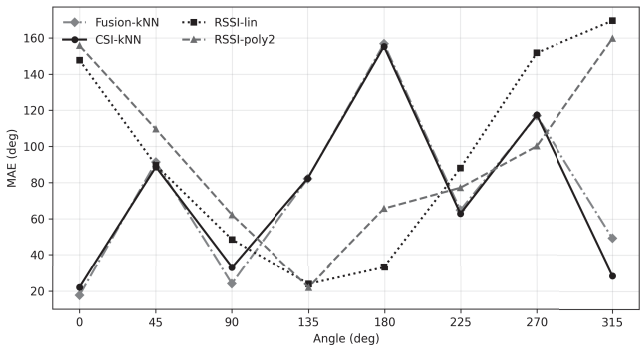

Fig. 2. Per-angle MAE for pooled out-of-fold predictions. The error varies strongly by azimuth sector, which indicates directional structure without a uniform full-circle mapping.

V. Discussion

Under experiment-wise all-angle evaluation, the present single-antenna ESP32-S3 geometry does not reach stable practical azimuth precision, even in one room, one LoS scenario, and a fixed 8-angle design. At the same time, the new results are more informative than the earlier partial-angle split because they show where the geometry does and does not carry useful directional structure. The CSI-based models improve aggregate MAE by about 18–20 deg over the RSSI regressors, but the improvement is not uniform across the circle. The best errors occur near 0, 90, and 315 deg, whereas 180 and 270 deg remain difficult. This means that the present setup exposes sector-dependent cues rather than a stable full-circle azimuth mapping. The same conclusion is consistent with edge-oriented Wi-Fi sensing surveys [3]: once sensing moves onto constrained devices, deployment conditions, signal-processing choices, and repeatable evaluation remain as important as model choice.

Compared with prior CSI/RSSI fingerprinting papers and broader CSI capability studies [4]–[6] and with commodity-WLAN AoA work [7], [8], the present setup lacks the richer preprocessing, multi-node or array geometry, and broader evaluation surface used in stronger reported localization or AoA results. The present result therefore bounds the current reliability envelope of single-antenna ESP32-S3 capture for this task.

Two limits bound the interpretation. First, the evidence still covers only one room and one LoS scenario. Second, experiment-wise evaluation is available for only 2 experiments, so the result is still an initial repeated-session characterization rather than a final generalization statement.

The results indicate that further progress is more likely to come from broader changes in study design than from regressor substitution alone. Relevant directions include richer measurement geometries, coordinated multi-receiver configurations, improved feature representations, and stricter repeated-session evaluation. Coordinated use of multiple ESP32-S3 or similar receivers with one antenna per node is one possible realization of that broader research program. For later extensions, a more promising path may be coordinated embedded sensing in which resource-constrained receivers contribute lightweight local descriptors to a shared coordinator rather than relying only on a single raw stream. Under that view, progress depends not only on richer geometry but also on stable configuration policies that limit control churn across sessions and on principled search over channel, placement, and synchronization settings when the added coordination cost is justified.

The interpretation of the result is also defined by the evaluation protocol. In a small embedded dataset, packet-mixed evaluation can reward memorization of capture conditions more than generalization across repeated sessions. By holding out one full experiment at a time, the present result remains tied to the current sensing geometry rather than to packet-level reuse across sessions. The same logic should be preserved in subsequent studies so that any gain can be attributed to richer observation geometry or improved representations rather than to a looser evaluation scheme.

VI. Conclusion

This paper contributes a controlled single-antenna ESP32-S3 azimuth-sensing study under integrity-aware experiment-wise evaluation, together with quantitative bounds for this measurement geometry over the full 8-angle set. The study covers 4796 valid packets from 16 capture subsets, 2 experiments, and 8 nominal angle points. Across pooled out-of-fold predictions from the 2 experiment-wise folds, the best MAE is 73.8 deg and the best within-10-degree rate is 28.1%, both achieved by CSI-kNN. The results show that the present geometry carries angle-dependent directional structure, but they still do not support stable practical azimuth sensing over the full circle. The characterization achieved in this paper will be useful for further research on embedded azimuth estimation,

including richer sensing geometries, revised feature representations, stricter repeated-session designs, and coordinated low-cost receiver configurations.

ACKNOWLEDGMENT

The paper draws on materials and intermediate results from the project "Intelligent Methods and Tools for Designing Modules for Autonomous Cyber-Physical Systems" (state registration No. 0124U002340, 2024–2028, Lviv Polytechnic National University).

REFERENCES

[1] Espressif Systems, "ESP-IDF Programming Guide: Wi-Fi channel state information," [Online]. Available at: https://docs.espressif.com/projects/esp-idf/en/stable/esp32s3/api-guides/wifi.html#wi-fi-channel-state-information, 2026, accessed: 2026-02-28.

[2] J. A. Armenta-Garcia, F. F. Gonzalez-Navarro, J. Caro-Gutierrez, and C. I. Garcia-Reyes, "Tools and methods for achieving wi-fi sensing in embedded devices," *Sensors*, vol. 25, no. 19, p. 6220, 2025. [Online]. Available: https://doi.org/10.3390/s25196220

[3] S. M. Hernandez and E. Bulut, "Wifi sensing on the edge: Signal processing techniques and challenges for real-world systems," *IEEE Communications Surveys and Tutorials*, vol. 25, no. 1, pp. 46–76, 2023. [Online]. Available: https://doi.org/10.1109/COMST.2022.3209144

[4] J. Wang and J. Park, "An enhanced indoor positioning algorithm based on fingerprint using fine-grained csi and rssi measurements of ieee 802.11n wlan," *Sensors*, vol. 21, no. 8, p. 2769, 2021. [Online]. Available: https://doi.org/10.3390/s21082769

[5] F. Abuhoureyah, W. Yan Chiew, A. S. Bin Mohd Isira, and M. Al-Andoli, "Free device location independent wifi-based localisation using received signal strength indicator and channel state information," *IET Wireless Sensor Systems*, vol. 13, no. 5, pp. 163–177, 2023. [Online]. Available: https://doi.org/10.1049/wss2.12065

[6] M. Cominelli, F. Gringoli, and F. Restuccia, "Exposing the csi: A systematic investigation of csi-based wi-fi sensing capabilities and limitations," in *2023 IEEE International Conference on Pervasive Computing and Communications (PerCom)*, 2023, pp. 81–90. [Online]. Available: https://doi.org/10.1109/PERCOM56429.2023.10099368

[7] T. Fukushima, T. Murakami, H. Abeysekera, T. Fujihashi, T. Watanabe, and S. Saruwatari, "Feasibility study of practical aoa estimation using compressed csi on commercial wlan devices," *IEEE Access*, vol. 10, pp. 49 128–49 141, 2022. [Online]. Available: https://doi.org/10.1109/ACCESS.2022.3159332

[8] X. Zhang, Y. Zhang, G. Liu, and T. Jiang, "Autoloc: Toward ubiquitous aoa-based indoor localization using commodity wifi," *IEEE Transactions on Vehicular Technology*, vol. 72, no. 6, pp. 8049–8060, 2023. [Online]. Available: https://doi.org/10.1109/TVT.2023.3243912

[9] M. Diadiuk and V. Pavlenko, "Design and experimental evaluation of CSI and RSSI-based indoor Wi-Fi ranging on ESP32-S3," *Information and Communication Technologies, Electronic Engineering*, vol. 6, no. 1, pp. 86–100, 2026. [Online]. Available: https://doi.org/10.23939/ictee2026.01.086

[10] Sage-Cat, "csi_capturing_example: ESP32 CSI/RSSI capture toolkit," [Online]. Available at: https://github.com/Sage-Cat/csi_capturing_example, 2026, gitHub repository; experiment release tag 'experiment/distance-estimation/2026-02-23T11-05-30Z'; accessed: 2026-03-10.